THE JOURNAL OF BIOLOGICAL CHEMISTRY VOL. 290, NO. 33, pp. 20374–20386, August 14, 2015

Staphylococcus aureus PerR Is a Hypersensitive Hydrogen Peroxide Sensor using Iron-mediated Histidine Oxidation*

Received for publication, May 16, 2015, and in revised form, June 27, 2015 Published, JBC Papers in Press, July 1, 2015, DOI 10.1074/jbc.M115.664961

Chang-Jun Ji[‡1], Jung-Hoon Kim[‡1], Young-Bin Won[‡], Yeh-Eun Lee[‡], Tae-Woo Choi[‡], Shin-Yeong Ju[‡], Hwan Youn[§], John D. Helmann[¶2], and Jin-Won Lee[‡3]

From the [‡]Department of Life Science and Research Center for Natural Sciences, Hanyang University, Seoul 133-791, Republic of Korea, the [§]Department of Biology, California State University Fresno, Fresno, California 93740-8034, and the [¶]Department of Microbiology, Cornell University, Ithaca, New York 14853-8101

Background: PerR is a metal-dependent H_2O_2 sensor in many Gram-positive bacteria.
Results: *Staphylococcus aureus* $PerR_{SA}$, previously known as a Mn^{2+}-specific repressor, uses Fe^{2+} to sense very low levels of H_2O_2.
Conclusion: The apparent lack of Fe^{2+}-dependent repressor activity of $PerR_{SA}$ is due to the hypersensitivity of $PerR_{SA}$ under aerobic conditions.
Significance: Cells expressing hypersensitive $PerR_{SA}$ are less virulent than those expressing $PerR_{BS}$.

In many Gram-positive bacteria PerR is a major peroxide sensor whose repressor activity is dependent on a bound metal cofactor. The prototype for PerR sensors, the *Bacillus subtilis* $PerR_{BS}$ protein, represses target genes when bound to either Mn^{2+} or Fe^{2+} as corepressor, but only the Fe^{2+}-bound form responds to H_2O_2. The orthologous protein in the human pathogen *Staphylococcus aureus*, $PerR_{SA}$, plays important roles in H_2O_2 resistance and virulence. However, $PerR_{SA}$ is reported to only respond to Mn^{2+} as corepressor, which suggests that it might rely on a distinct, iron-independent mechanism for H_2O_2 sensing. Here we demonstrate that $PerR_{SA}$ uses either Fe^{2+} or Mn^{2+} as corepressor, and that, like $PerR_{BS}$, the Fe^{2+}-bound form of $PerR_{SA}$ senses physiological levels of H_2O_2 by iron-mediated histidine oxidation. Moreover, we show that $PerR_{SA}$ is poised to sense very low levels of endogenous H_2O_2, which normally cannot be sensed by *B. subtilis* $PerR_{BS}$. This hypersensitivity of $PerR_{SA}$ accounts for the apparent lack of Fe^{2+}-dependent repressor activity and consequent Mn^{2+}-specific repressor activity under aerobic conditions. We also provide evidence that the activity of $PerR_{SA}$ is directly correlated with virulence, whereas it is inversely correlated with H_2O_2 resistance, suggesting that $PerR_{SA}$ may be an attractive target for the control of *S. aureus* pathogenesis.

Reactive oxygen species, which are produced endogenously as a by-product of aerobic metabolism or exogenously by microbial competitors and eukaryotic hosts, can cause oxidative stress to bacteria by damaging cellular constituents (1, 2). To cope with reactive oxygen species, bacteria have evolved sophisticated oxidative stress response systems including transcription factors that efficiently sense specific reactive oxygen species and induce appropriate defense systems (2–4). For example, OxyR in the Gram-negative model bacterium *Escherichia coli* senses H_2O_2 using cysteine oxidation, and activates transcription of ~20 genes, including genes involved in H_2O_2 detoxification (1). Whereas many Gram-negative bacteria use OxyR as the major H_2O_2 sensor, many Gram-positive bacteria use PerR as a functional equivalent of OxyR (5, 6).

Bacillus subtilis PerR ($PerR_{BS}$)[4] is a member of Fur family of metal-dependent regulators and is the prototype for a group of metal-dependent peroxide sensing repressors (5). $PerR_{BS}$ contains a structural Zn^{2+} coordinated by four cysteine residues (Cys_4:Zn site, Site 1) and a second regulatory metal binding site (Site 2) composed of three N-donor ligands (His-37, His-91, and His-93) and two O-donor ligands (Asp-85 and Asp-104). Although the binding of either Fe^{2+} ($PerR_{BS}$:Zn,Fe) or Mn^{2+} ($PerR_{BS}$:Zn,Mn) at Site 2 activates $PerR_{BS}$ to bind DNA, only $PerR_{BS}$:Zn,Fe can sense low levels of H_2O_2. Unlike cysteine thiol-based peroxide sensors such as OxyR and OhrR, $PerR_{BS}$ senses H_2O_2 by metal-catalyzed histidine oxidation. Reaction of Fe^{2+}, bound to Site 2, with H_2O_2 leads to the rapid oxidation of either His-37 or, to a lesser degree, His-91 (two of the Site 2 ligands) with concomitant loss of iron binding (7). Structurally, this results in an opening of the DNA-binding competent caliper-like conformation, leading to a loss of DNA binding and thus allowing the induction of genes that are normally repressed by active $PerR_{BS}$:Zn,Fe (8).

Staphylococcus aureus is a major human pathogen commonly causing nosocomial and community-acquired infectious diseases worldwide. *S. aureus*, which can be found as part of the normal skin flora and in anterior nares of the nasal passages, can cause a spectrum of illnesses from minor skin and soft tissue

* This work was supported, in whole or in part, by National Institutes of Health Grant GM059323 (to J. D. H.) and National Research Foundation of Korea (NRF) grants funded by the Korea government (MSIP) Grants NRF-2011-0017199 and NRF-2009-0068133 (to J.-W. L.). The authors declare that they have no conflict of interest.
[1] Both authors contributed equally to this work.
[2] To whom correspondence may be addressed. Tel.: 607-255-6570; Fax: 607-255-3904; E-mail: jdh9@cornell.edu.
[3] To whom correspondence may be addressed. Tel.: 82-2-2220-0952; Fax: 82-2-2299-3495; E-mail: jwl@hanyang.ac.kr.

[4] The abbreviations used are: $PerR_{BS}$, *B. subtilis* PerR; $PerR_{SA}$, *S. aureus* PerR; MLMM, metal-limited minimal medium; PAR, 4-(2-pyridylazo)resorcinol; FA, fluorescence anisotropy; Tricine, *N*-[2-hydroxy-1,1-bis(hydroxymethyl)ethyl]glycine.

infections to more invasive and serious diseases such as pneumonia, meningitis, osteomyelitis, endocarditis, toxic shock syndrome, bacteremia, and sepsis (9). As a facultative anaerobic Gram-positive bacterium, *S. aureus* also uses PerR for the control of oxidative stress response (10, 11). The *S. aureus* PerR ($PerR_{SA}$) regulon is similar to that described for $PerR_{BS}$ and includes genes encoding KatA, AhpCF, MrgA, Fur, and PerR, as well as others encoding thioredoxin reductase (TrxB), bacterioferritin comigratory protein (Bcp), and an iron storage protein ferritin (Ftn). Despite the similarity of the H_2O_2-dependent regulation of the $PerR_{SA}$ regulon, Fe^{2+} was reported to be completely ineffective as a corepressor for the $PerR_{SA}$-regulated genes, which were only repressed by Mn^{2+}. Indeed, expression of the $PerR_{SA}$-regulated genes is induced rather than repressed by added Fe^{2+} (11–14). These observations led to the conclusion that $PerR_{SA}$ is a Mn^{2+}-specific repressor and further suggest that $PerR_{SA}$ may use a fundamentally different and iron-independent mechanism to sense H_2O_2. Despite the importance of $PerR_{SA}$ in the regulation of virulence factors of *S. aureus*, the mechanism by which $PerR_{SA}$ senses H_2O_2 has not been elucidated.

Here we have analyzed the metal-dependent H_2O_2 sensing mechanisms of $PerR_{SA}$ *in vitro* and *in vivo* in comparison with those of $PerR_{BS}$. $PerR_{SA}$, like many other Fur family proteins, contains a structural Zn^{2+} site coordinated by four cysteine residues, which is resistant to oxidation by physiologically relevant H_2O_2 concentration. Contrary to the suggestion that $PerR_{SA}$ is a Mn^{2+}-specific repressor, the regulatory metal binding site (composed of His-43, Asp-91, His-97, His-99, and Asp-110) can bind Fe^{2+} even with higher affinity than Mn^{2+} when measured under anaerobic conditions. Moreover, the Fe^{2+}-bound $PerR_{SA}$, but not the Mn^{2+}-bound form, can sense H_2O_2 by Fe^{2+}-dependent oxidation of His-43 and His-97. In cells grown under aerobic conditions most of $PerR_{SA}$ is detected in the fully oxidized state, whereas cells grown under oxygen-limited conditions exhibit Fe^{2+}-dependent repression of the $PerR_{SA}$ regulon. The exquisite sensitivity of $PerR_{SA}$ to inactivation likely explains the previous observation of an apparent lack of Fe^{2+}-dependent repressor activity. Finally, we provide evidence that the high H_2O_2 sensitivity of $PerR_{SA}$ (in comparison to $PerR_{BS}$) is important for H_2O_2 resistance under aerobic conditions and that the low sensitivity of $PerR_{BS}$ (in comparison to $PerR_{SA}$) increases virulence of *S. aureus* in host.

Experimental Procedures

Bacterial Strains, Media, and Growth Conditions—The bacterial strains used in this study are listed in Table 1. *E. coli*, *B. subtilis*, and *S. aureus* were grown in Luria-Bertani (LB) media at 37 °C with appropriate antibiotics unless otherwise indicated. As metal-limited minimal media (MLMM), MOPS-buffered minimal medium was used for *B. subtilis* (15), and phosphate-buffered minimal medium was used for *S. aureus* (10). Oxygen-limited cultures were grown in 15-ml rubber screw-top tubes with the addition of 0.2% potassium nitrate. To facilitate oxygen-limited growth of *S. aureus* in MLMM, 1% Chelex-treated tryptone was added.

TABLE 1
Strains used in this study

Strains	Relevant genotype and feature	Source
S. aureus		
Newman	Wild type, human clinical isolate	NCTC
RN451	RN450 lysogenic for Φ11	NARSA
RN4220	Restriction-deficient transformation recipient	NARSA
LS0085	Newman *perR*::*cat*	This study
LS0088	LS0085 pLL29::$perR_{SA}$-*FLAG*	This study
LS0093	LS0085 pLL29	This study
LS0106	Newman pCN33::P_{mrgA}-*lacZ*	This study
LS0107	Newman pCN33::P_{katA}-*lacZ*	This study
LS0111	LS0085 pLL29::$perR_{SA}$-*FLAG* pCN33::P_{mrgA}-*lacZ*	This study
LS0114	LS0085 pLL29::$perR_{BS}$-*FLAG* pCN33::P_{mrgA}-*lacZ*	This study
LS0124	LS0085 pLL29 pCN33::P_{mrgA}-*lacZ*	This study
LS0134	LS0085 pLL29:: $perR_{BS}$-*FLAG*	This study
LS0166	LS0085 pCN48::$perR_{SA}$-*FLAG*	This study
LS0241	LS0085 pLL29::$perR_{SA}$-*FLAG* pCN33::P_{katA}-*lacZ*	This study
LS0242	LS0085 pLL29::$perR_{SA}$ *(H43A)-FLAG* pCN33::P_{katA}-*lacZ*	This study
LS0243	LS0085 pLL29::$perR_{SA}$ *(H97A)-FLAG* pCN33::P_{katA}-*lacZ*	This study
LS0244	LS0085 pLL29::$perR_{SA}$ *(C102S)-FLAG* pCN33::P_{katA}-*lacZ*	This study
LS0245	LS0085 pLL29 pCN33::P_{katA}-*lacZ*	This study
LS0304	LS0085 pLL29::$perR_{SA}$ *(D91A)-FLAG* pCN33::P_{katA}-*lacZ*	This study
LS0305	LS0085 pLL29::$perR_{SA}$ *(H99A)-FLAG* pCN33::P_{katA}-*lacZ*	This study
LS0306	LS0085 pLL29::$perR_{SA}$ *(C105S)-FLAG* pCN33::P_{katA}-*lacZ*	This study
LS0307	LS0085 pLL29::$perR_{SA}$ *(D110A)-FLAG* pCN33::P_{katA}-*lacZ*	This study
LS0308	LS0085 pLL29::$perR_{SA}$ *(C142S)-FLAG* pCN33::P_{katA}-*lacZ*	This study
LS0309	LS0085 pLL29::$perR_{SA}$ *(C145S)-FLAG* pCN33::P_{katA}-*lacZ*	This study
B. subtilis		
HB9703	*perR*::*tet*	Ref. 15
HB9738	HB9703 *amyE*::$perR_{BS}$-*FLAG SPβC2Δ2*::*Tn917*::Φ (P_{mrgA}-*cat-lacZ*)	Ref. 15
LB1530	HB9703 *amyE*::$perR_{SA}$-*FLAG SPβC2Δ2*::*Tn917*::Φ (P_{mrgA}-*cat-lacZ*)	This study
LB1532	HB9703 *amyE*::*spc SPβC2Δ2*::*Tn917*::Φ (P_{mrgA}-*cat-lacZ*)	This study
E. coli		
HE9501	BL21 (DE3) pLysS pET-16b::$perR_{BS}$	Ref. 15
LE0003	BL21 (DE3) pLysS pET-16b::$perR_{SA}$	This study
LE0031	BL21 (DE3) pLysS pET-16b::$perR_{SA}$ *(H43A)*	This study
LE0032	BL21 (DE3) pLysS pET-16b::$perR_{SA}$ *(D91A)*	This study
LE0033	BL21 (DE3) pLysS pET-16b::$perR_{SA}$ *(H97A)*	This study
LE0034	BL21 (DE3) pLysS pET-16b::$perR_{SA}$ *(H99A)*	This study
LE0035	BL21 (DE3) pLysS pET-16b::$perR_{SA}$ *(C102S)*	This study
LE0036	BL21 (DE3) pLysS pET-16b::$perR_{SA}$ *(C105S)*	This study
LE0037	BL21 (DE3) pLysS pET-16b::$perR_{SA}$ *(D110A)*	This study
LE0038	BL21 (DE3) pLysS pET-16b::$perR_{SA}$ *(C142S)*	This study
LE0039	BL21 (DE3) pLysS pET-16b::$perR_{SA}$ *(C145S)*	This study
LE2302	BL21 (DE3) pLysS pET-11a::$oxyR_{EC}$	This study

Construction of a perR Deletion Mutant Strain of S. aureus Newman—The $perR_{SA}$::*cat* cassette was constructed by joining PCR using two 1-kb DNA fragments (upstream and downstream of $perR_{SA}$ ORF) and a fragment with a chloramphenicol resistance marker (*cat*) from pDG1661. This cassette was cloned into the BamHI and EcoRI sites of pMAD (16) having a

temperature-sensitive replication origin and a erythromycin-resistant marker (*em*) resulting in pJL954. Then, pJL954 was introduced into *S. aureus* Newman (NCTC8178) after passage through a restriction-deficient host *S. aureus* RN4220. *S. aureus* Newman strain having pJL954 integrated into the chromosome by a Campbell-type event was selected based on light blue colony color on LB agar plates containing chloramphenicol, erythromycin, and X-Gal after growing cells at 43 °C. After an overnight subculture two times in LB broth containing chloramphenicol at 30 °C, erythromycin-sensitive but chloramphenicol-resistant colonies were selected on LB plate at 43 °C. After confirmation of $perR_{SA}$ deletion by PCR, the resultant strain was named LS0085.

Construction of perR-FLAG Fusion and Reporter Fusion in B. subtilis and S. aureus—For the expression of $perR_{SA}$-*FLAG* fusion in *B. subtilis*, the PCR fragment containing $perR_{SA}$ ORF and about 200 bp upstream region was cloned into BamHI and EagI sites of pJL070 (15) generating pJL361. The ScaI digest of pJL361 was introduced to the *perR* null mutant *B. subtilis* strain HB9703 (15) to generate a transformant containing $perR_{SA}$-*FLAG* in the *amyE* locus. Then the P_{mrgA}-*cat-lacZ* reporter fusion stain (LB1530) was constructed by transduction with SPβ phage from HB1122 (17). For the expression of $perR_{SA}$-*FLAG* or $perR_{BS}$-*FLAG* fusions in *S. aureus*, the DNA fragment of pJL070 containing $perR_{BS}$-*FLAG* and that of pJL361 containing $perR_{SA}$-*FLAG*, were each cloned into BamHI and EcoRI sites of pLL29 (18) producing pJL1434 and pJL1430, respectively. Mutant alleles of $perR_{SA}$-*FLAG* were generated by the QuikChange method (Stratagene) using pJL1430 as templates. Each of these plasmids was integrated into the chromosome of *S. aureus* RN4220 with the help of *int* gene encoded in pLL2787, and then transferred into the *perR* null mutant *S. aureus* Newman strain (LS0085) by phage transduction using Φ11 (19). For the construction of reporter fusion plasmids, the *lacZ* gene from pDG1661 was PCR-amplified with the introduction of an NcoI site just after the KpnI site, and cloned into the KpnI and EcoRI sites of pCN33 resulting in pJL901. Then, DNA fragment containing the *mrgA* or *katA* promoter regions was introduced into the BamHI and NcoI sites of pJL901. The resulting reporter fusion plasmids were introduced into *S. aureus* Newman by electroporation after passage through *S. aureus* RN4220. To increase the copy number of $perR_{SA}$-*FLAG*, $perR_{SA}$-*FLAG* was cloned into the BamHI and EcoRI sites of the high copy number plasmid pCN48 (20) resulting in pJL643. This plasmid was introduced into the *perR* null mutant *S. aureus* Newman (LS0085) by electroporation after passage through *S. aureus* RN4220, generating a strain named LS0166. $PerR_{BS}$-FLAG and $PerR_{SA}$-FLAG proteins are fully functional as judged by reporter fusion assays, and were used for complementation of the *perR* null mutant strains and pulldown assays (15, 21).

Overexpression and Purification of Proteins—The PCR-amplified DNA fragments containing the $perR_{SA}$ ORF were digested with BspHI and BamHI, and cloned into the NcoI and BamHI sites of pET-16b (Novagen) producing a plasmid named pJL203. Mutant alleles of $perR_{SA}$ were generated by the QuikChange method (Stratagene) using pJL203 as template. *E. coli oxyR* was cloned into the NdeI and BamHI sites of pET-11a (Novagen) producing a plasmid named pJL1282. The encoded proteins were overexpressed using *E. coli* BL21(DE3) pLysS cells. Wild type (WT) $PerR_{SA}$ proteins were purified after overexpression in *E. coli* BL21(DE3) pLysS cells harboring pJL203 as previously described for $PerR_{BS}$ proteins (15). Briefly, the cell lysates were clarified by centrifugation and then $PerR_{SA}$ was purified by heparin-Sepharose and Mono-Q chromatography using buffer A (20 mM Tris-HCl, pH 8.0, 0.1 M NaCl, and 5% glycerol (v/v)) containing 10 mM EDTA with the application of a linear gradient of 0.1–1 M NaCl. Further purification was performed using a Superdex-200 (HiLoad 16/60) column equilibrated with Chelex-treated buffer A. The concentration of $PerR_{SA}$ was determined using a molar extinction coefficient of 10,430 M^{-1} cm^{-1} at 280 nm.

Enzyme Assays—On-gel catalase activity was assayed using 1:1 mixture of 5% ferric chloride and 5% potassium ferricyanide after gel-soaking in 2 mM H_2O_2. β-Galactosidase assays were performed with or without 100 μM H_2O_2 treatment for 30 min as described previously (15), except that lysostaphin (10 μg/ml) was used for the lysis of *S. aureus* cells. Measurement of Zn^{2+} release by H_2O_2 was performed as described previously (15) using 2.5 μM dimeric $PerR_{SA}$ and 100 μM 4-(2-pyridylazo)resorcinol (PAR). The Zn^{2+} content of purified $PerR_{SA}$ by PAR assay was measured using a molar extinction coefficient of 85,000 M^{-1} cm^{-1} at 494 nm for Zn^{2+}-PAR complex (15).

Western Blot Analysis—At A_{600} = 0.6, 10-ml cultures were harvested by centrifugation after the addition of 1.1 ml of trichloroacetic acid. Then, cells were resuspended in 500 μl of 10% trichloroacetic acid and sonicated. After recovering sonicated samples by centrifugation, the pellets were resuspended with 60 μl of alkylating buffer (100 mM iodoacetamide, 0.5 M Tris, pH 8.0, 5% glycerol, 100 mM NaCl, 2% SDS) and incubated for 1 h in the dark to alkylate-free thiols. Alkylated samples of 10 μl (75 μg of protein) were separated on 13.3% non-reducing SDS-PAGE gel using a Tris-Tricine buffer system and blotted to a polyvinylidene difluoride membrane. FLAG-tagged proteins were probed with mouse monoclonal anti-FLAG antibody and anti-mouse antibody conjugated with alkaline phosphatase (Sigma).

Fluorescence Anisotropy (FA) Experiments—FA experiments were performed using an LS55 luminescence spectrometer (PerkinElmer Life Sciences) installed in an anaerobic chamber (Coy). A 6-carboxyfluorescein (6-FAM)-labeled *katA*-PerR box DNA fragment was generated by annealing 5′-6-FAM-TTAAATTATAATTATTATAAATTGT-3′ (Integrated DNA Technology) and its unlabeled complement. FA measurements (λ_{ex} = 492 nm, slit width = 15 nm; λ_{em} = 520 nm, slit width = 20 nm, integration time = 1 s) were performed in 3 ml of Chelex-treated anaerobic buffer A. The percentage activity and K_d for DNA of purified $PerR_{SA}$ were determined to be ~20% and ~1 nM, respectively, by titration of $PerR_{SA}$ into 3 ml of buffer A containing 10 nM DNA and 1 mM manganese as reported previously (7). For the metal binding and H_2O_2 sensitivity assays, buffer A containing 100 nM DNA and 100 nM active dimeric $PerR_{SA}$ were used, and FA was measured after each addition.

MALDI-TOF and LC-ESI MS/MS Mass Analyses—To analyze *in vivo* oxidation of $PerR_{SA}$ (Fig. 4), LS0166 cells expressing

$PerR_{SA}$-FLAG were grown in MLMM containing 50 μM $FeSO_4$ or 50 μM $MnCl_2$. At an A_{600} of ~1, cells were treated with or without 100 μM H_2O_2 for 2 min and lysed with 50 μg of lysostaphin for 1 h in 0.5 ml of buffer A. $PerR_{SA}$-FLAG protein recovered using anti-FLAG M2-agarose beads (Sigma) was incubated with 100 mM iodoacetamide in the presence of 50 mM EDTA and 1% SDS for 1 h in the dark, and separated on SDS-PAGE gel. The protein bands corresponding to $PerR_{SA}$-FLAG were analyzed by MALDI-TOF MS using a 4700 Proteomics Analyzer instrument (Applied Biosystems) after in-gel tryptic digestion as described previously (15, 22). The MALDI-TOF MS analysis of *in vitro* oxidation of purified $PerR_{SA}$ (Fig. 3*D*) was performed as described previously (7, 15) using a Voyager-DE STR instrument (Applied Biosystems). The analysis of protein oxidation after overexpression in *E. coli* (Fig. 5) was performed as previously described (22), except that sample preparations for Fig. 5*B* were carried out in an anaerobic chamber. The sites of oxidation were identified by LC-MS/MS analyses using an Agilent nanoflow-1200 series HPLC system connected to a linear ion trap mass spectrometer (Thermo Scientific).

Caenorhabditis elegans Killing Assay—NGM agar plates (5.5 cm diameter) spread with 30 μl of A_{600} = 1 culture of *E. coli* OP50 (laboratory nematode food), *S. aureus* expressing no PerR (LS0093), *S. aureus* expressing $PerR_{SA}$ (LS0088), or *S. aureus* expressing $PerR_{BS}$ (LS0134) were used. For each assay 90 L4 stage *C. elegans* were used in triplicate of 30 worms/plate. The plates were incubated at 25 °C, and scored for live and dead worms at least every 24 h as described previously (23). For each assay, the survival of worms was calculated by the Kaplan-Meier method, and survival differences were tested by using OASIS (24).

Results

Structural Zn^{2+} and Regulatory Metal Binding Sites of $PerR_{SA}$—$PerR_{SA}$ is highly similar (67% sequence identity) to $PerR_{BS}$, but previous results have highlighted some striking differences in their response to added metal ions (11–14). To provide a structural context for our investigation of $PerR_{SA}$ reactivity we generated a homology model of $PerR_{SA}$ based on the known structure of $PerR_{BS}$ (25). As shown in Fig. 1, *A* and *B*, $PerR_{SA}$ retains four highly conserved cysteine residues (Cys-102, Cys-105, Cys-142, and Cys-145) corresponding to those involved in high affinity structural Zn^{2+} binding (Site 1) in most Fur family proteins as well as in $PerR_{BS}$ (5, 15, 26). $PerR_{SA}$ also has five other residues (His-43, Asp-91, His-97, His-99, and Asp-110), which correspond to the N/O donor ligands for the regulatory metal binding (Site 2) in $PerR_{BS}$ (7, 8). To investigate the role of these predicted metal-binding residues in protein function, we generated $PerR_{SA}$ mutants and examined the *in vivo* repressor activities of WT and mutants using a PerR-regulated *katA* promoter-*lacZ* fusion (P_{katA}-*lacZ*) (Fig. 1*C*). As expected, the P_{katA}-*lacZ* reporter fusion was repressed in cells expressing WT $PerR_{SA}$-FLAG but derepressed in the *perR* null mutant cells. Note that the repression levels of P_{katA}-*lacZ* reporter fusion by WT $PerR_{SA}$-FLAG were similar to those observed with the WT *S. aureus* strain, indicating that the *perR* null mutant strain complemented with WT $PerR_{SA}$-FLAG behaves like WT strain. All nine mutants exhibited no repressor activity for the P_{katA}-*lacZ* reporter fusion, and furthermore, these mutant proteins were present at levels greater than WT protein (Fig. 1*D*) indicative of a loss of repression of the autoregulated *perR* promoter. These results indicate that these amino acid residues proposed to be metal ligands are essential for *in vivo* repressor function.

Previously we have demonstrated that the structural Zn^{2+} binding status of $PerR_{BS}$ can be monitored by mobility difference on non-reducing SDS-PAGE: monomeric $PerR_{BS}$ containing bound Zn^{2+} migrates faster than $PerR_{BS}$ lacking bound Zn^{2+} (15). To investigate the Zn^{2+} binding status of $PerR_{SA}$, WT and mutant proteins were separated on SDS-PAGE after overexpression in *E. coli*. WT and Site 2 mutants migrated with the mobility characteristic of the Zn^{2+}-bound form, whereas all four Site 1 mutants migrated with the mobility characteristic of the Zn^{2+}-lacking form (Fig. 1*E*). This result indicates that $PerR_{SA}$ contains a tightly bound Zn^{2+} coordinated by four cysteine residues, and that mutations at the proposed regulatory metal binding site do not affect the Zn^{2+} binding.

$PerR_{SA}$ was shown previously to be a Mn^{2+}-specific repressor, which suggested that this protein might use an Fe^{2+}-independent H_2O_2 sensing mechanism (11, 14). We therefore wondered whether the cysteine residues coordinating Zn^{2+} might serve a role in peroxide sensing. To test this, we measured the rate of Zn^{2+} release from purified $PerR_{SA}$ upon H_2O_2 treatment (Fig. 1*F*) by monitoring the formation of a Zn^{2+}-PAR complex as reported previously (15). The second-order rate constant of Zn^{2+} release and the Zn^{2+} content of $PerR_{SA}$ were determined to be ~0.05 M^{-1} s^{-1} and ~0.8 Zn^{2+}/monomer, respectively, which are comparable with those of $PerR_{BS}$ (15). The slow rate of H_2O_2-mediated Zn^{2+} release, along with the retention of Zn^{2+} despite the use of 10 mM EDTA during the purification procedures, further supports the idea that the Zn^{2+} site of $PerR_{SA}$ plays a structural rather than a peroxide sensing role. All these data together indicate that $PerR_{SA}$ has a structural Zn^{2+} site coordinated by four cysteine residues and a regulatory metal binding site composed of His-43, Asp-91, His-97, His-99, and Asp-110.

In Vivo Repressor Activity of $PerR_{SA}$ in Comparison with $PerR_{BS}$—To investigate the difference in metal- and H_2O_2-sensing ability of $PerR_{BS}$ and $PerR_{SA}$, the repressor activities of PerR proteins were examined in MLMM using an *mrgA* promoter *lacZ*-fusion (P_{mrgA}-*lacZ*). As reported previously, $PerR_{BS}$ repressed the P_{mrgA}-*lacZ* reporter fusion in the presence of either Fe^{2+} or Mn^{2+}, and Fe^{2+}-dependent repression was relieved upon H_2O_2 treatment (Fig. 2*A*) (7). $PerR_{SA}$ repressed the P_{mrgA}-*lacZ* reporter fusion in the presence of Mn^{2+} but not in the presence of Fe^{2+}, consistent with the previous finding that $PerR_{SA}$ is a Mn^{2+}-dependent repressor (Fig. 2*B*) (11). Interestingly, however, β-galactosidase expression was increased by about 2-fold in the presence of Fe^{2+} as reported previously (12) and further increased upon H_2O_2 treatment. The previous observation that this Fe^{2+}-dependent induction of the *mrgA* gene is not observed with the *perR* null mutant *S. aureus* (12) suggests that the Fe^{2+}- and H_2O_2-dependent increase of β-galactosidase expression is mediated by $PerR_{SA}$,

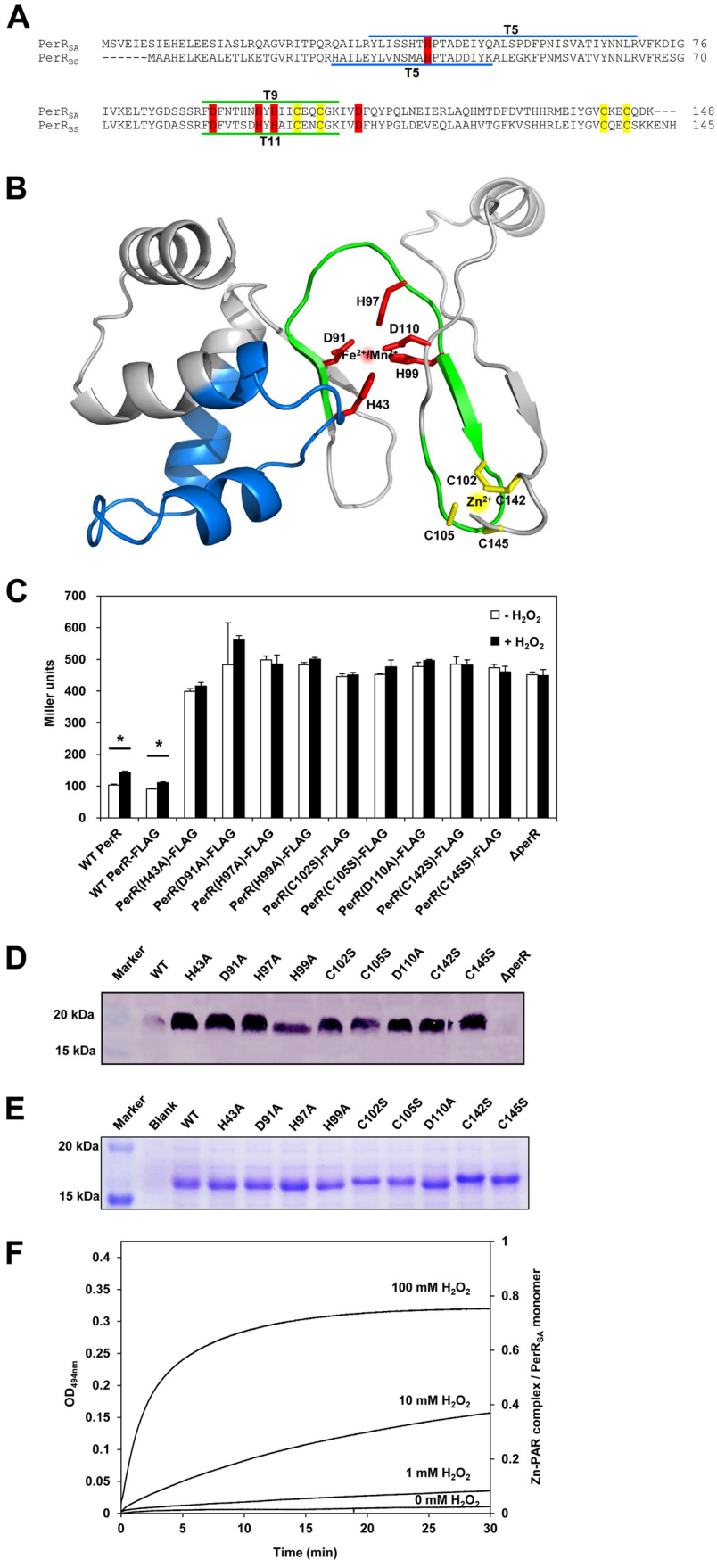
A
T5
PerR$_{SA}$ MSVEIESIEHELEESIASLRQAGVRITPQRQAILRYLISSHTHPTADEIYQALSPDFPNISVATIYNNLRVFKDIG 76
PerR$_{BS}$ ------MAAHELKEALETLKETGVRITPQRHAILEYLVNSMAHPTADDIYKALEGKFPNMSVATVYNNLRVFRESG 70
T5
T9
PerR$_{SA}$ IVKELTYGDSSSRFEFNTHNHYHIICEQCGKIVDFQYPQLNEIERLAQHMTDFDVTHHRMEIYGVCKECQDK--- 148
PerR$_{BS}$ LVKELTYGDASSRFEFVTSDHYHAICENCGKIVDFHYPGLDEVEQLAAHVTGFKVSHHRLEIYGVCQECSKKENH 145
T11
B
H97
D91
D110
Fe2+/Mn2+
H99
H43
C102
Zn2+ C142
C105
C145
C
Miller units
- H2O2
+ H2O2
WT PerR
WT PerR-FLAG
PerR(H43A)-FLAG
PerR(D91A)-FLAG
PerR(H97A)-FLAG
PerR(H99A)-FLAG
PerR(C102S)-FLAG
PerR(C105S)-FLAG
PerR(D110A)-FLAG
PerR(C142S)-FLAG
PerR(C145S)-FLAG
ΔperR
D
Marker
WT
H43A
D91A
H97A
H99A
C102S
C105S
D110A
C142S
C145S
ΔperR
20 kDa
15 kDa
E
Marker
Blank
WT
H43A
D91A
H97A
H99A
C102S
C105S
D110A
C142S
C145S
20 kDa
15 kDa
F
100 mM H2O2
10 mM H2O2
1 mM H2O2
0 mM H2O2
OD494nm
Zn-PAR complex / PerRSA monomer
Time (min)

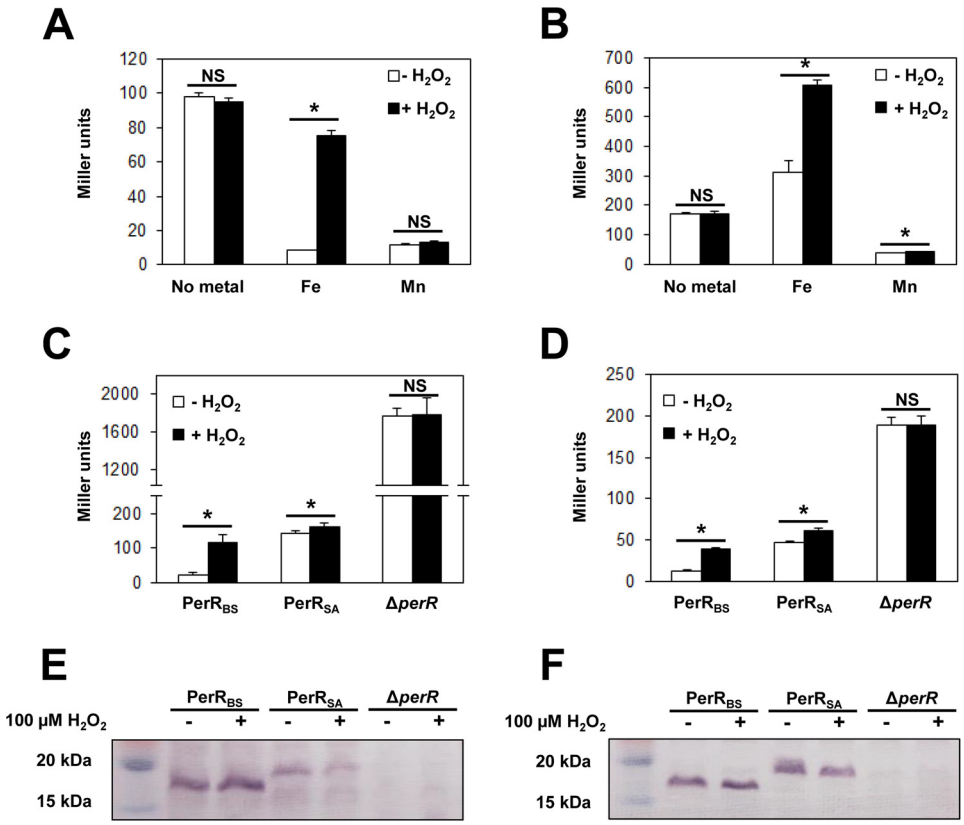

FIGURE 2. **Comparison of activities between $PerR_{SA}$ and $PerR_{BS}$ *in vivo*.** *A* and *B*, metal-dependent repressor activities of $PerR_{BS}$ (*A*) and $PerR_{SA}$ (*B*). *B. subtilis* cells expressing $PerR_{BS}$-FLAG (HB9738) and *S. aureus* cells expressing $PerR_{SA}$-FLAG (LS0111) were grown aerobically in MLMM supplemented with 10 μM $FeSO_4$ or 10 μM $MnCl_2$, and treated with 100 μM H_2O_2 ($+H_2O_2$) for 30 min or not ($-H_2O_2$). Repressor activities of $PerR_{BS}$ and $PerR_{SA}$ were measured using *B. subtilis* P_{mrgA}-*lacZ* and *S. aureus* P_{mrgA}-*lacZ* reporter fusions, respectively. Statistical analysis was performed with a Student's *t* test (*, $p < 0.05$; *NS*, not significant). *C* and *D*, repressor activities of $PerR_{BS}$ and $PerR_{SA}$ in *B. subtilis* (*C*) and in *S. aureus* (*D*). *B. subtilis* cells expressing no PerR (LB1532), $PerR_{BS}$-FLAG (HB9738), or $PerR_{SA}$-FLAG (LB1530), and *S. aureus* cells expressing no PerR (LS0124), $PerR_{BS}$-FLAG (LS0114), or $PerR_{SA}$-FLAG (LS0111) were used. Cells were grown aerobically in LB medium and treated with 100 μM H_2O_2 ($+H_2O_2$) for 30 min or not ($-H_2O_2$). Repressor activities of PerR proteins in *B. subtilis* were measured using *B. subtilis* P_{mrgA}-*lacZ* and those in *S. aureus* were measured using *S. aureus* P_{mrgA}-*lacZ* reporter fusions. *A–D*, repressor activities were expressed as Miller units of β-galactosidase activity (values represent the mean ± S.D. from three separate experiments). Statistical analysis was performed with a Student's *t* test (*, $p < 0.05$; *NS*, not significant). *E* and *F*, Western blot analysis of $PerR_{BS}$ and $PerR_{SA}$ in *B. subtilis* (*E*) and in *S. aureus* (*F*). *B. subtilis* cells expressing no PerR (LB1532), $PerR_{BS}$-FLAG (HB9738), or $PerR_{SA}$-FLAG (LB1530), and *S. aureus* cells expressing no PerR (LS0124), $PerR_{BS}$-FLAG (LS0114), or $PerR_{SA}$-FLAG (LS0111) were used. Cells were grown aerobically in LB medium and treated with 100 μM H_2O_2 ($+H_2O_2$) for 30 min or not ($-H_2O_2$). The FLAG-tagged PerR proteins were probed by anti-FLAG antibody.

although it is not clear whether Fe^{2+} directly interacts with $PerR_{SA}$ or not.

To test whether differences in cellular milieu between *B. subtilis* and *S. aureus* affect the repressor activity of PerR proteins, $PerR_{BS}$ and $PerR_{SA}$ were expressed both in *B. subtilis* (Fig. 2, *C* and *E*) and *S. aureus* (Fig. 2, *D* and *F*). $PerR_{BS}$ expressed in *S. aureus* repressed the *S. aureus* P_{mrgA}-*lacZ* reporter fusion with even higher repressor activity than $PerR_{SA}$, and responded normally to H_2O_2 as in *B. subtilis* (Fig. 2*D*). $PerR_{SA}$ expressed in *B. subtilis* or in *S. aureus* repressed the *B. subtilis* P_{mrgA}-*lacZ* fusion or *S. aureus* P_{mrgA}-*lacZ* fusion, respectively, although not quite as efficiently as $PerR_{BS}$ (Fig. 2, *C* and *D*). Interestingly, the repression levels of both the *B. subtilis* and *S. aureus* P_{mrgA}-*lacZ* reporter fusions by $PerR_{SA}$ were similar to those by $PerR_{BS}$ treated with H_2O_2 for 30 min. Furthermore, $PerR_{SA}$ responded poorly to H_2O_2 (~1.2-fold induction) both in *B. subtilis* and *S. aureus* when compared with the responsiveness of $PerR_{BS}$ to H_2O_2 (more than 3-fold induction). Thus it is likely that the

FIGURE 1. **Metal binding sites of $PerR_{SA}$.** *A*, sequence alignment of $PerR_{SA}$ with $PerR_{BS}$. The candidate ligands for Zn^{2+} (*yellow*) and Fe^{2+}/Mn^{2+} (*red*) are conserved in $PerR_{SA}$. The two tryptic peptides of $PerR_{SA}$, T5 (*blue*) containing His-43 and T9 (*green*) containing His-97, are the sites of oxidation. The tryptic peptides of $PerR_{BS}$, T5 containing His-37 and T11 containing His-91, are also shown. *B*, predicted structure of $PerR_{SA}$ monomer based on $PerR_{BS}$ structure (Protein Data Bank code 3F8N) (25) using Swiss Model (40). *C*, mutational analyses of $PerR_{SA}$. Wild type *S. aureus* cells (WT PerR, LS0107), *S. aureus* cells expressing no $PerR_{SA}$ (Δ*perR*, LS0245), or *S. aureus* cells expressing $PerR_{SA}$-FLAG variants as indicated, were grown in LB medium and treated with 100 μM H_2O_2 ($+H_2O_2$) for 30 min or not ($-H_2O_2$). Repressor activities of $PerR_{SA}$ variants were measured using P_{katA}-*lacZ* reporter fusion and were expressed as Miller units of β-galactosidase activity (values represent the mean ± S.D. from three separate experiments). Statistical analysis was performed with a Student's *t* test (*, $p < 0.05$). *D*, analysis of expression levels for $PerR_{SA}$ variants. *S. aureus* cells, expressing no $PerR_{SA}$ (Δ*perR*) or expressing $PerR_{SA}$-FLAG variants as indicated, were grown in LB medium. The expression levels of FLAG-tagged PerR variants were analyzed by Western blot using anti-FLAG antibody. *E*, structural Zn^{2+}-binding assay of $PerR_{SA}$ variants on SDS-PAGE gel. The crude extracts of *E. coli* cells, overexpressing no $PerR_{SA}$ (*Blank*) or overexpressing $PerR_{SA}$ variants as indicated, were preincubated with 10 mM DTT and separated by SDS-PAGE using Tris glycine buffer system. Protein bands were detected by Coomassie Brilliant Blue R staining. *F*, oxidation of Cys_4:Zn site by H_2O_2. Release of Zn^{2+} from $PerR_{SA}$:Zn (5 μM purified $PerR_{SA}$) was measured by monitoring Zn^{2+}-PAR complex at 494 nm after treatment of 0, 1, 10, and 100 mM H_2O_2 as described previously (15). The Zn^{2+} content was calculated using a molar extinction coefficient of 85,000 M^{-1} cm^{-1} at 494 nm for Zn^{2+}-PAR complex (15).

difference in responsiveness to metal and H_2O_2 between $PerR_{SA}$ and $PerR_{BS}$ is due to differences between the PerR proteins rather than the cellular environments. In summary the *in vivo* data indicate that Fe^{2+} addition appears to lead to apparent activation or derepression, rather than repression, of $PerR_{SA}$-regulated genes under our experimental conditions.

In Vitro $PerR_{SA}$ Senses H_2O_2 by Iron-mediated Histidine Oxidation—To test whether $PerR_{SA}$ is activated to bind DNA by both Mn^{2+} and Fe^{2+}, we measured the apparent affinity of $PerR_{SA}$ for Fe^{2+} and Mn^{2+} using a fluorescence anisotropy-based DNA-binding assay (Fig. 3*A*). Because PerR is immediately oxidized in the presence of Fe^{2+} under aerobic conditions as reported previously (7), all the FA experiments were performed under anaerobic conditions. Consistent with the observed Mn^{2+}-dependent repressor activity of $PerR_{SA}$ *in vivo*, the DNA-binding affinity of $PerR_{SA}$ was increased by the addition of Mn^{2+}. The apparent K_d for the Mn^{2+}-dependent activation of $PerR_{SA}$ was determined to be 9 μM, which is slightly weaker than that of $PerR_{BS}$ (~3 μM). Interestingly, despite the apparent lack of Fe^{2+}-dependent repressor activity of $PerR_{SA}$ *in vivo*, Fe^{2+} could also increase the DNA binding of $PerR_{SA}$ in a concentration-dependent manner. The apparent K_d for the Fe^{2+}-pendent activation of $PerR_{SA}$ (0.1 μM) appeared to be the same as that of $PerR_{BS}$. These results therefore suggest that the apparent lack of Fe^{2+}-dependent repressor activity and poor responsiveness to H_2O_2 of $PerR_{SA}$ *in vivo* is not due to a decreased Fe^{2+} binding affinity of $PerR_{SA}$ *per se*.

Because both Fe^{2+} and Mn^{2+} increase the DNA binding affinity of $PerR_{SA}$, we next investigated the effect of H_2O_2 on the DNA-binding activity of different metal-bound forms of $PerR_{SA}$ ($PerR_{SA}$:Zn,Fe and $PerR_{SA}$:Zn,Mn) under anaerobic conditions (Fig. 3, *B* and *C*). Upon addition of 10 μM H_2O_2, $PerR_{SA}$:Zn,Fe completely lost DNA-binding activity in 20 s, whereas $PerR_{SA}$:Zn,Mn retained DNA-binding activity for 10 min even in the presence of 1 mM H_2O_2, indicating that $PerR_{SA}$ utilizes Fe^{2+}, but not Mn^{2+}, for the sensing of low levels of H_2O_2 *in vitro*. Furthermore, loss of the DNA-binding ability of $PerR_{SA}$:Zn,Fe by H_2O_2 treatment could not be restored by the addition of Mn^{2+}, indicating that H_2O_2 sensing by $PerR_{SA}$:Zn,Fe likely accompanies protein modification rather than simply the loss of bound Fe^{2+}.

To test the hypothesis that H_2O_2 leads to a metal-dependent modification of $PerR_{SA}$, we analyzed the effect of H_2O_2 on different metallated forms of $PerR_{SA}$ using MALDI-TOF MS (Fig. 3*D*). $PerR_{SA}$:Zn,Mn displayed no detectable changes in tryptic peptide peaks after 100 μM H_2O_2 treatment. However, H_2O_2-treated $PerR_{SA}$:Zn,Fe exhibited a significant decrease in the intensity of the T5 peptide (Tyr-36 to Arg-70) and T9* peptide (Phe-90 to Lys-107) with a concomitant increase in the intensity of two tryptic peptides corresponding to T5 + 16 and T9* + 16. The sites of oxidation responsible for this 16-Da mass increase were mapped to His-43 (corresponding to His-37 in $PerR_{BS}$) in the T5 peptide and His-97 (corresponding to His-91 in $PerR_{BS}$) in the T9* peptide using LC-ESI MS analysis (Fig. 1*A* and data not shown). Note that the T9* peptide also contains Cys-102 and Cys-105, which were detected in their fully alkylated form, indicative of no oxidation at cysteine residues after 100 μM H_2O_2 treatment, consistent with the structural role for

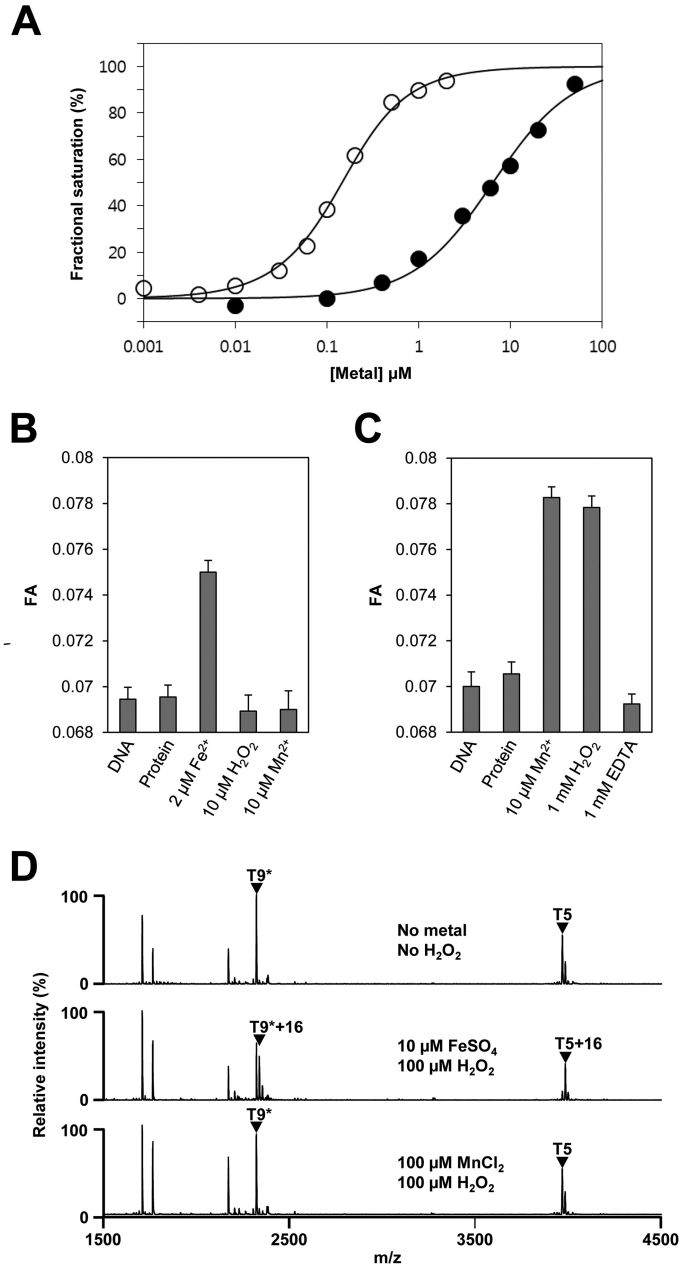

FIGURE 3. **Metal-dependent DNA binding and H_2O_2-mediated oxidation of $PerR_{SA}$ *in vitro*.** *A*, metal-dependent DNA binding activity of $PerR_{SA}$. Various concentrations of metal ions (*open circle* for Fe^{2+} and *filled circle* for Mn^{2+}) are added to samples containing 100 nM DNA and 100 nM active $PerR_{SA}$ dimer, and metal-dependent DNA-binding of $PerR_{SA}$ was monitored by fluorescence anisotropy change. *B*, sensitivity of $PerR_{SA}$ to H_2O_2 in the presence of Fe^{2+}. Protein (100 nM active $PerR_{SA}$:Zn dimer), $FeSO_4$, H_2O_2, and $MnCl_2$ were sequentially added to buffer A containing 100 nM DNA with an interval of 2 min between each addition, and FA was measured after each addition. 10 μM H_2O_2 rapidly (<20 s) inactivated $PerR_{SA}$ in the presence of 2 μM Fe^{2+} and the loss of $PerR_{SA}$ activity was not recovered by the addition of Mn^{2+}. *C*, sensitivity of $PerR_{SA}$ to H_2O_2 in the presence of Mn^{2+}. Protein (100 nM active $PerR_{SA}$:Zn dimer), $MnCl_2$, H_2O_2, and EDTA were sequentially added to buffer A containing 100 nM DNA with an interval of 2 min between each addition except for 10 min between H_2O_2 and EDTA, and FA was measured after each addition. $PerR_{SA}$ was insensitive to 1 mM H_2O_2 for 10 min but lost DNA-binding activity rapidly by addition of 1 mM EDTA. *D*, metal-dependent oxidation of $PerR_{SA}$. Oxidation of $PerR_{SA}$ by H_2O_2 in the presence of 10 μM Fe^{2+} or 100 μM Mn^{2+} was monitored by MALDI-TOF MS after tryptic digestion. Note that no cysteine oxidation was observed as judged by fully alkylated T9 peptide (T9*) containing Cys-102 and Cys-105.

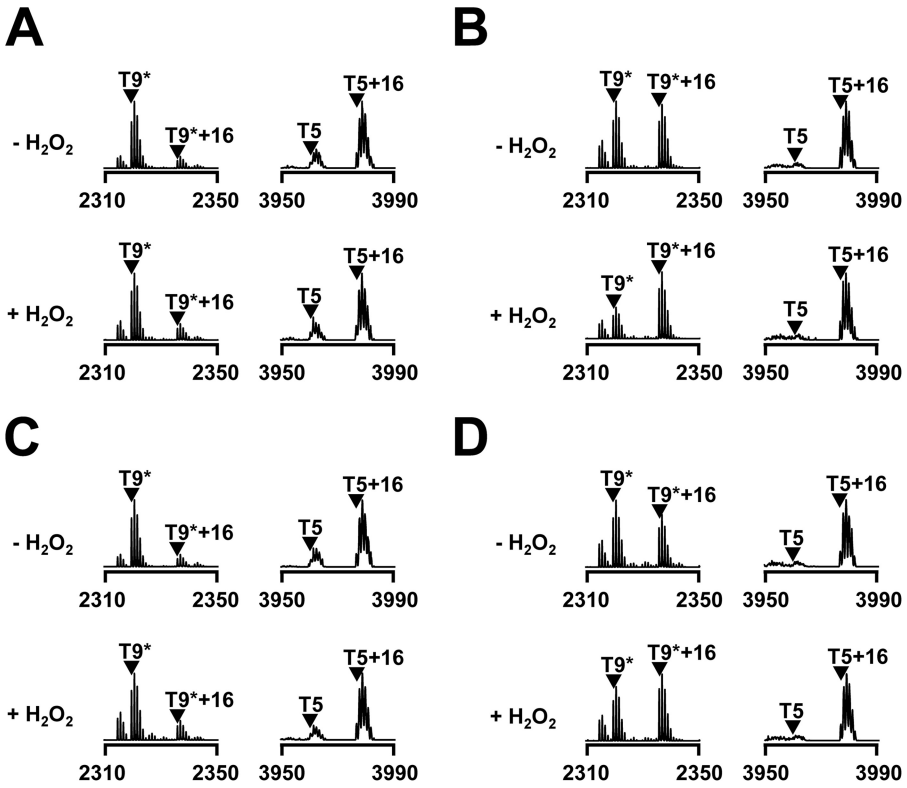

FIGURE 4. ***In vivo* oxidation of $PerR_{SA}$.** Oxidation of $PerR_{SA}$ from *S. aureus* cells (LS0166) grown aerobically in MLMM supplemented with no metal ion (*A*), 50 μM $FeSO_4$ (*B*), 50 μM $MnCl_2$ (*C*), or both 50 μM $FeSO_4$ and 50 μM $MnCl_2$ (*D*). $PerR_{SA}$-FLAG proteins were recovered by immunoprecipitation from *S. aureus* cells treated with no H_2O_2 or 100 μM H_2O_2 for ~2 min, and analyzed by MALDI-TOF MS after SDS-PAGE separation and in-gel tryptic digestion.

these zinc-coordinating cysteine residues. These data indicate that $PerR_{SA}$, like $PerR_{BS}$, senses low levels of H_2O_2 by Fe^{2+}-mediated oxidation of either of two histidine residues, His-43 and/or His-97, which are used as regulatory metal binding ligands.

Apparent Lack of Fe^{2+}-dependent Repressor Activity of $PerR_{SA}$ in Vivo Is Due to the Hypersensitivity of $PerR_{SA}$ to Iron-mediated Oxidation under Aerobic Conditions—Since we observed the Fe^{2+}-dependent DNA-binding activity and Fe^{2+}-mediated histidine oxidation of $PerR_{SA}$ *in vitro*, we wondered whether H_2O_2 sensing by histidine oxidation would also occur *in vivo*. To monitor the oxidation of $PerR_{SA}$ *in vivo*, we analyzed the oxidation status of $PerR_{SA}$ recovered by immunoprecipitation from *S. aureus* cells grown in MLMM supplemented with Fe^{2+} or Mn^{2+} using MALDI-TOF MS (Fig. 4). Interestingly, even without H_2O_2 treatment, almost all of the T5 peptide was detected as oxidized form (T5 + 16) and a significant amount of the T9* peptide was also detected as oxidized form (T9* + 16) for $PerR_{SA}$ from cells grown in MLMM supplemented with Fe^{2+} or both Fe^{2+} and Mn^{2+}. However, less oxidation was observed at both T5 and T9* peptides for $PerR_{SA}$ from cells grown in MLMM supplemented with Mn^{2+} or no metal ion, and no significant further oxidation of these peptides was detected upon H_2O_2 treatment. These observations indicate that under aerobic growth conditions the majority of $PerR_{SA}$:Zn,Fe exists in an oxidized form even without external addition of H_2O_2.

To compare the sensitivity of $PerR_{SA}$ with those of well known H_2O_2 sensors, *E. coli* OxyR and $PerR_{BS}$, we analyzed protein oxidation in *E. coli* using MALDI-TOF MS as described previously (22). As noted for $PerR_{SA}$ recovered from *S. aureus* cells (Fig. 4), $PerR_{SA}$ from aerobically grown *E. coli* cells exhibited a significant oxidation at the T5 peptide even in the absence of H_2O_2 treatment (Fig. 5*A*). However, $PerR_{SA}$ from *E. coli* cells grown under oxygen-limited conditions exhibited no detectable oxidation at both T5 and T9* peptides, and oxidation of these peptides was observed upon external H_2O_2 treatment (Fig. 5*B*). In contrast, under aerobic conditions, $PerR_{BS}$ exhibited less oxidation at both T5 and T11* peptides when compared with $PerR_{SA}$ (Fig. 5*C*), and *E. coli* OxyR exhibited no detectable oxidation of both T19 and T20 peptides, which contain the peroxidatic cysteine (Cys-199) and resolving cysteine (Cys-208), respectively (Fig. 5*D*). These results indicate that $PerR_{SA}$ is more sensitive than $PerR_{BS}$ or *E. coli* OxyR to oxidation by low levels of H_2O_2, which are normally encountered during the aerobic growth of *E. coli*.

The above observations suggest that the poor H_2O_2 responsiveness and the apparent lack of Fe^{2+}-dependent repressor activity of $PerR_{SA}$ can be overcome under oxygen-limited growth conditions where limited amounts of H_2O_2 are generated. Consistent with this hypothesis, $PerR_{SA}$ exhibited an increased repressor activity under oxygen-limited growth conditions (Fig. 6*A*) when compared with that under aerobic growth conditions (Fig. 2*D*). Furthermore, under these conditions $PerR_{SA}$ responded to H_2O_2 (~3-fold induction) much like $PerR_{BS}$, as judged by an increased β-galactosidase activity upon H_2O_2 treatment. We also investigated the metal-dependent

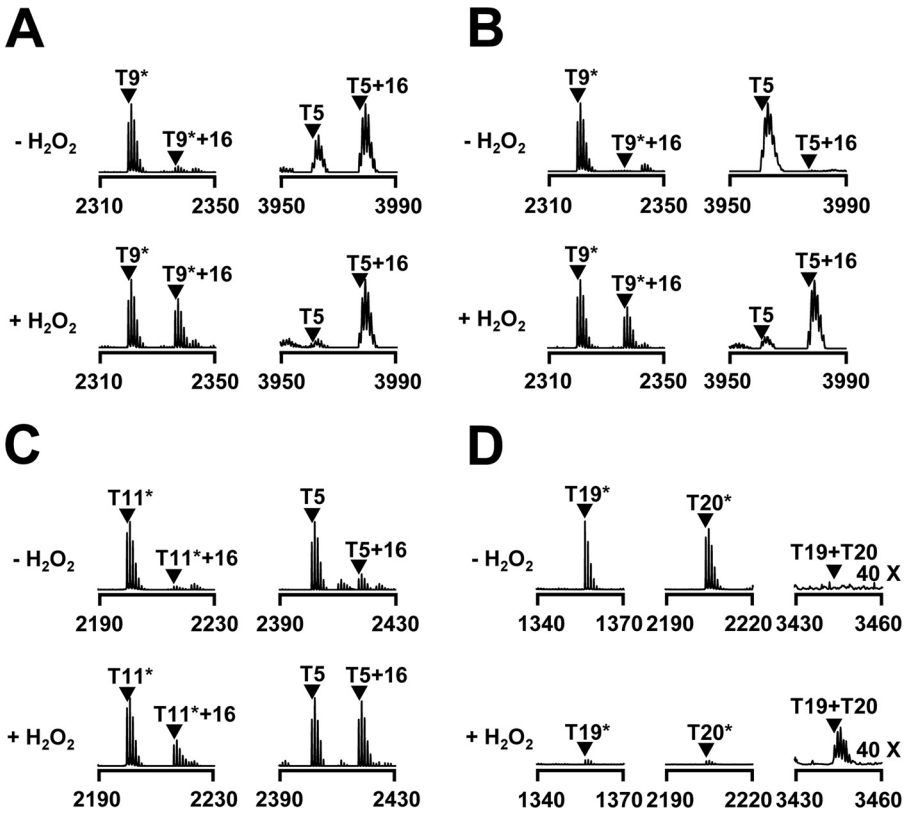

FIGURE 5. **Comparison of oxidation sensitivity among $PerR_{BS}$, *E. coli* OxyR and $PerR_{SA}$.** Oxidation of $PerR_{SA}$ (*A*), $PerR_{BS}$ (*C*), or *E. coli* OxyR (*D*) in *E. coli* cells (LE0003, $PerR_{SA}$; HE9501, $PerR_{BS}$; LE2302, *E. coli* OxyR) grown under aerobic conditions, or $PerR_{SA}$ (*B*) in *E. coli* cells (LE0003) grown under oxygen-limited conditions. *E. coli* cells were grown in LB media under aerobic conditions or oxygen-limited conditions, and treated with or without 100 μM H_2O_2 for 1 min. Oxidation status of proteins was analyzed by MALDI-TOF MS after SDS-PAGE fractionation and in-gel tryptic digestion as reported previously (22). *Asterisks* represent peptides containing carboxyamidomethylated cysteine residue(s).

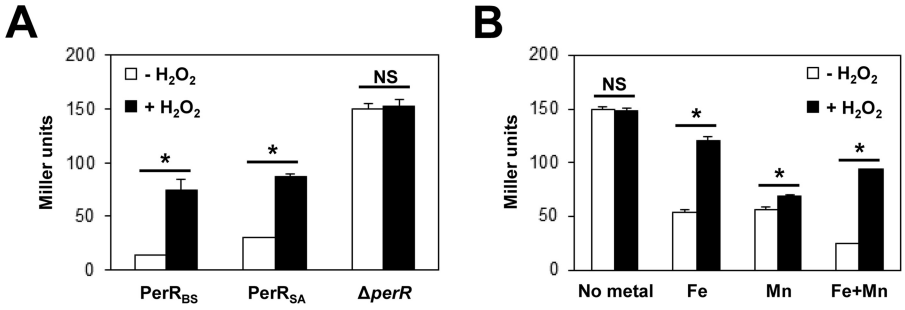

FIGURE 6. ***In vivo* repressor activities of $PerR_{SA}$ under oxygen-limited conditions.** *A*, repressor activities and H_2O_2 sensing abilities of $PerR_{BS}$ and $PerR_{SA}$ under oxygen-limited conditions. *S. aureus* cells expressing no PerR (LS0124), $PerR_{BS}$-FLAG (LS0114), or $PerR_{SA}$-FLAG (LS0111) were grown in LB medium under oxygen-limited conditions, and treated with 100 μM H_2O_2 ($+H_2O_2$) for 30 min or not ($-H_2O_2$). Repressor activities of PerR proteins were measured using *S. aureus* P_{mrgA}-*lacZ* reporter fusions. *B*, metal-dependent repressor activities of $PerR_{SA}$ under oxygen-limited conditions. *S. aureus* cells expressing $PerR_{SA}$-FLAG (LS0111) were grown in MLMM supplemented with no metal ion, 10 μM $FeSO_4$, 10 μM $MnCl_2$, or both 10 μM $FeSO_4$ and 10 μM $MnCl_2$ under oxygen-limited conditions, and treated with 100 μM H_2O_2 ($+H_2O_2$) for 30 min or not ($-H_2O_2$). Repressor activities were measured using *S. aureus* P_{mrgA}-*lacZ* reporter fusion. *A* and *B*, repressor activities were expressed as Miller units of β-galactosidase activity (values represent the mean $\pm$ S.D. from three separate experiments). Statistical analysis was performed with a Student's *t* test (*, $p < 0.05$; *NS*, not significant).

H_2O_2-sensing ability of $PerR_{SA}$ by growing cells in MLMM under oxygen-limited growth conditions. As shown in Fig. 6*B*, addition of either Fe^{2+} or Mn^{2+} enabled $PerR_{SA}$ to repress the P_{mrgA}-*lacZ* reporter fusion, and β-galactosidase activity was increased by more than 2-fold upon H_2O_2 treatment in the presence of Fe^{2+} or in the presence of both Fe^{2+} and Mn^{2+}, but only slightly (~1.2-fold) in the presence of only Mn^{2+}. These data demonstrate that $PerR_{SA}$ functions as a Fe^{2+}-dependent repressor and senses H_2O_2 in an Fe^{2+}-dependent manner *in vivo* under oxygen-limited growth conditions (Fig. 6), as observed *in vitro* under anaerobic conditions (Fig. 3). We also note that the efficient sensing of H_2O_2 in the presence of both Fe^{2+} and Mn^{2+} is consistent with the higher affinity of $PerR_{SA}$ for Fe^{2+} than Mn^{2+} as observed *in vitro* (Fig. 3*A*). In general, these results indicate that $PerR_{SA}$ behaves in oxygen-limited cells much like $PerR_{BS}$ does in *B. subtilis*, and that the apparent lack of Fe^{2+}-dependent repressor activity (and thus poor H_2O_2 responsiveness) of $PerR_{SA}$ under aerobic conditions is due to an efficient oxidation of $PerR_{SA}$ by low levels of endogenous H_2O_2.

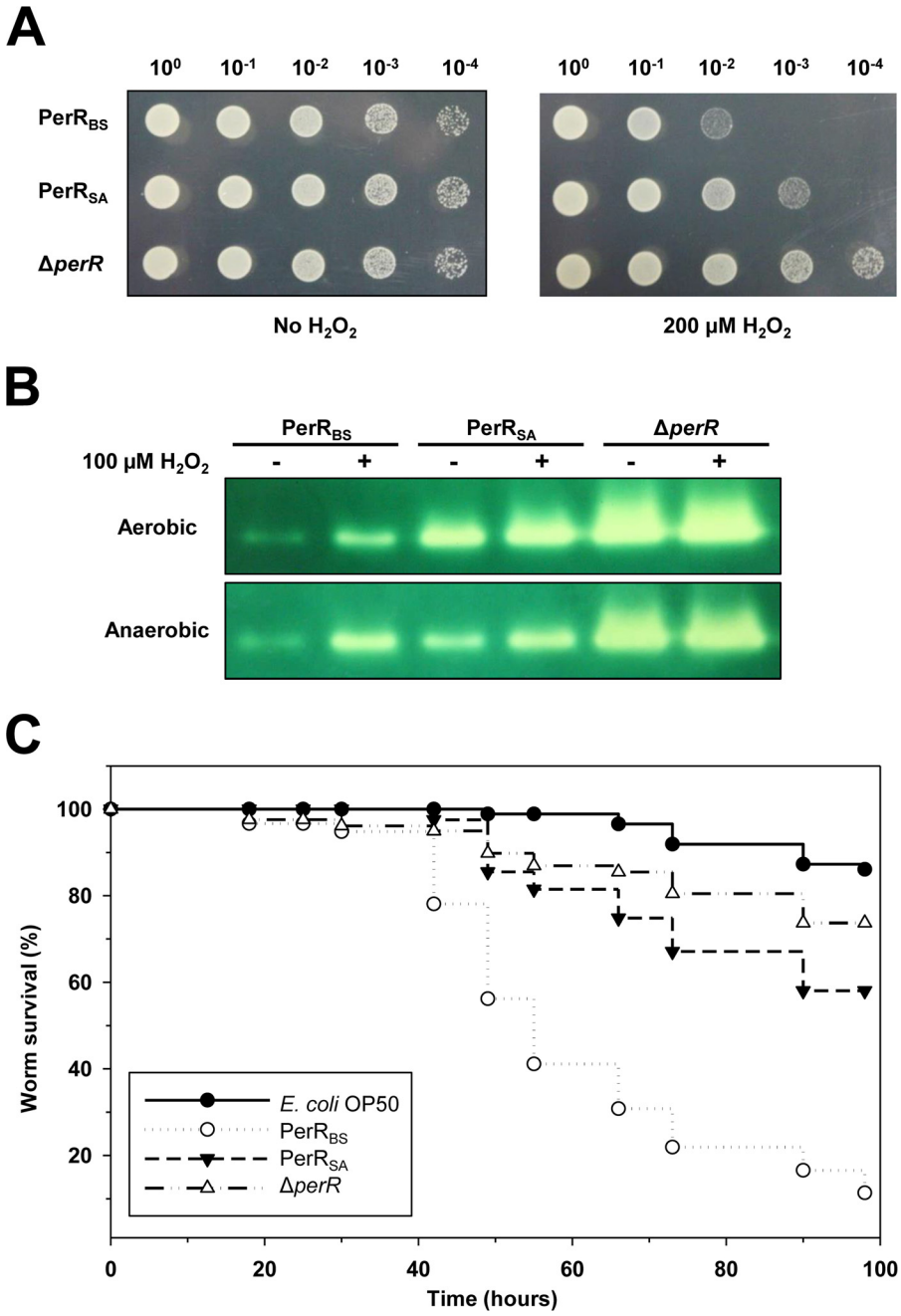

FIGURE 7. **Effects of PerR activity on H_2O_2 resistance and virulence of *S. aureus*.** *A*, effects of PerR activity on the survival of *S. aureus* in the absence or presence of H_2O_2. *S. aureus* cells (3 μl of A_{600} = 1 culture, with indicated dilutions) expressing no PerR (LS0093), $PerR_{BS}$-FLAG (LS0134), or $PerR_{SA}$-FLAG (LS0088) were spotted on LB-agar plate containing no H_2O_2 or 200 μM H_2O_2, and grown under aerobic conditions at 37 °C. Note that fresh LB agar plate shielded from light was used to prevent the generation of H_2O_2 by photochemical reactions (41). *B*, effects of PerR activity on the expression of KatA. *S. aureus* cells expressing no PerR (LS0093), $PerR_{BS}$-FLAG (LS0134), or $PerR_{SA}$-FLAG (LS0088) were grown in LB medium under either aerobic or oxygen-limited conditions, and treated with 100 μM H_2O_2 or not. Catalase activity staining was performed after separation of cell extract (10 μg protein) on native PAGE gel. *C*, effects of PerR activity on the pathogenicity of *S. aureus* using *C. elegans* as a model host. *C. elegans* killing was presented as Kaplan-Meier survival plots of worms fed with *E. coli* OP50 (negative control) (n = 86), *S. aureus* strain expressing no PerR (LS0093) (n = 86), $PerR_{BS}$-FLAG (LS0134) (n = 77), or $PerR_{SA}$-FLAG (LS0088) (n = 84).

Fe^{2+}-mediated H_2O_2 Susceptibility of $PerR_{SA}$ Is Important for H_2O_2 Resistance and Pathogenicity of S. aureus—It has been suggested that resistance to oxidative stress is an important factor for the survival and persistence of *S. aureus* (14). To investigate whether the difference in sensitivity of PerR proteins to oxidation affects the H_2O_2 resistance of *S. aureus*, we measured the growth of cells in the presence and absence of H_2O_2 (Fig. 7*A*). As expected the *perR* null mutant *S. aureus* cells exhibited an increased H_2O_2 resistance compared with those expressing $PerR_{SA}$. Also, compared with cells expressing $PerR_{SA}$, *S. aureus* cells expressing $PerR_{BS}$ (which is less sensitive to Fe-mediated oxidation than $PerR_{SA}$) exhibited an increased H_2O_2 sensitivity. These data indicate that the ability of $PerR_{SA}$ to respond to very low levels of H_2O_2 encountered during aerobic growth is important for the H_2O_2 resistance of *S. aureus*. Consistent with this, high levels of KatA activity were detected in the *perR* null mutant *S. aureus* cells, but low levels of KatA activity were detected

from cells expressing $PerR_{BS}$, when compared with those expressing $PerR_{SA}$ (Fig. 7*B*).

Although the H_2O_2 defense enzymes, such as KatA and AhpC, which are under the control of $PerR_{SA}$ play important roles in the nasal colonization and infection by *S. aureus*, it has been reported that they are not important for virulence (11, 14). However, interestingly, PerR is known to be required for virulence in other models of infection including murine skin abscess (11, 14), fruit fly (27), and zebrafish (28). We used a *C. elegans* model, which has been widely used as an invertebrate animal model for *S. aureus* pathogenesis (23), to investigate whether the difference in sensitivity of PerR proteins affects the virulence of *S. aureus* (Fig. 7*C*). As noted for other models of infection, the *perR* null mutant *S. aureus* was attenuated in the *C. elegans* model. Unexpectedly, *S. aureus* cells expressing $PerR_{BS}$ killed *C. elegans* more rapidly than did those expressing $PerR_{SA}$. These results suggest that the virulence of *S. aureus* is somewhat directly correlated with the activity of PerR, given that heterologous $PerR_{BS}$, which is less sensitive to oxidation than $PerR_{SA}$, increases the virulence of *S. aureus*.

Discussion

PerR and PerR-like regulators have been described in a wide variety of organisms since the first characterization in *B. subtilis* (4, 5, 17, 29, 30). However, to date, the H_2O_2-sensing mechanism of PerR proteins has only been extensively studied for $PerR_{BS}$ (7, 15, 21). Here we demonstrate that $PerR_{SA}$, previously regarded as a Mn^{2+}-specific repressor, senses H_2O_2 using the same Fe^{2+}-dependent histidine oxidation mechanism previously described for $PerR_{BS}$. Moreover we show that the apparent lack of Fe^{2+}-dependent repressor activity, and the consequent Mn^{2+}-specific repressor activity of $PerR_{SA}$ *in vivo*, is due to the hypersensitivity of $PerR_{SA}$ to H_2O_2 under aerobic conditions, rather than due to a decreased Fe^{2+} binding affinity of $PerR_{SA}$ *per se*.

Several lines of evidence indicate that $PerR_{SA}$ is a more sensitive H_2O_2 sensor than either $PerR_{BS}$ or *E. coli* OxyR. The majority of $PerR_{SA}$ in aerobically grown *S. aureus* is detected in an oxidized form (Fig. 4), whereas only partial oxidation is observed with $PerR_{BS}$ from aerobically grown *B. subtilis* (7). However, the interpretation of this result can be complicated by potential differences in the levels of endogenous H_2O_2 between these two species. Therefore, we directly compared the levels of oxidized PerR proteins when both were expressed in either *S. aureus* or *B. subtilis*. Indeed the direct measurement of KatA activity (Fig. 7*B*) and reporter fusion assays (Fig. 2, *C* and *D*) indicate that the expression levels of $PerR_{SA}$-regulated genes are higher in cells expressing $PerR_{SA}$ than in those expressing $PerR_{BS}$. This indicates that under otherwise identical conditions, oxidation levels of $PerR_{SA}$ are higher than those of $PerR_{BS}$ in both *B. subtilis* and *S. aureus*, consistent with the hypothesis that $PerR_{SA}$ is intrinsically more susceptible to oxidation than $PerR_{BS}$. Furthermore, we also used *E. coli*, where H_2O_2 detoxification systems are under the control of OxyR, as neutral host to directly compare the sensitivity of PerR proteins and OxyR protein. The rate of H_2O_2 generation in aerobically growing *E. coli* is ~10 μM per s (31), however, the steady-state concentration of H_2O_2 is kept ~50 nM by the action of scavenging enzymes such as AhpC (1). Normally, under these routine aerobic growth conditions, OxyR is inactive: OxyR is activated when the intracellular H_2O_2 concentration reaches ~200 nM (1, 32, 33). $PerR_{BS}$ has a second-order rate constant of $\sim 10^5\ M^{-1}\ s^{-1}$ for inactivation by H_2O_2, which is comparable with that of *E. coli* OxyR (7). Consistent with this, $PerR_{BS}$ and *E. coli* OxyR exhibit no significant oxidation in aerobically grown *E. coli* (Fig. 5, *C* and *D*). In contrast, a significant oxidation of $PerR_{SA}$ is observed in aerobically grown *E. coli* without external H_2O_2 treatment, indicating that endogenously produced H_2O_2 is sufficient to oxidize $PerR_{SA}$ (Fig. 5*A*). Collectively these indicate that $PerR_{SA}$ senses very low levels of H_2O_2 (as little as ~50 nM) as generated during normal aerobiosis in *E. coli*, levels that do not significantly oxidize $PerR_{BS}$ or *E. coli* OxyR. Corroborating with this, it has recently been reported that OxyR2 from *Vibrio vulnificus* is activated under normal aerobic growth conditions, whereas OxyR1, an *E. coli* OxyR homologue, is only activated by exogenous H_2O_2 (34).

The efficient sensing of H_2O_2 and induction of defense enzymes have been considered crucial for pathogens that have to fight against H_2O_2 assault by macrophages or neutrophils (35, 36). However, the *perR* null mutant *S. aureus* strain, which is more resistant to H_2O_2 than the wild type by constitutive expression of H_2O_2 defense enzymes, exhibits attenuated virulence in our *C. elegans* model of infection (Fig. 7*C*) as observed with other models of infection (11, 27, 28). Moreover, the H_2O_2-sensitive *S. aureus* strain by the expression of $PerR_{BS}$ (Fig. 7, *A* and *B*) is not attenuated in *C. elegans* (Fig. 7*C*), consistent with the previous finding that neither KatA nor AhpC are required for resistance to neutrophil-dependent killing or virulence of *S. aureus* (14). Instead, the expression of $PerR_{BS}$, which is less sensitive to H_2O_2 compared with $PerR_{SA}$, increases the virulence suggesting that the activity of PerR positively correlates with the virulence of *S. aureus*. This may imply that the inactivation of PerR by H_2O_2, rather than the direct poisoning of bacteria by H_2O_2, can be exploited by phagocytic cells that wish to reduce the virulence of *S. aureus*. It is not clear why inactivation of PerR activity reduces the virulence of *S. aureus*. One possible explanation would be poor growth of *S. aureus* in the iron-limited host environment. Derepression of PerR-regulon is likely to lead to Fe^{2+} deficiency due to the elevated expression of KatA, which consumes Fe^{2+}, and Fur, which represses Fe^{2+} uptake, as observed with *B. subtilis* (37). Alternatively, or in addition, active PerR may be involved in the induction of the virulence factor, either directly or indirectly. Indeed it has been shown that *Streptococcus pyogenes* PerR regulates an extracellular virulence factor, MF3, directly (38). All together, our findings that the activity of PerR is directly linked to the virulence of *S. aureus* suggests that $PerR_{SA}$ can be an attractive target for a novel approach to design new drugs for *S. aureus* treatment (39).

In contrast to virulence, H_2O_2 resistance is inversely correlated with the activity of PerR because the H_2O_2 defense systems are derepressed by H_2O_2-mediated PerR inactivation. Our results clearly show this relationship (Fig. 7, *A* and *B*). As reported previously the *perR* null mutant *S. aureus* exhibits increased resistance to H_2O_2, whereas *S. aureus* expressing $PerR_{BS}$ exhibits an increased sensitivity to H_2O_2 than that

expressing $PerR_{SA}$, presumably due to the hyper-repression of $PerR_{SA}$-regulated genes by $PerR_{BS}$. Although KatA and AhpC are not required for virulence, they are known to play important roles for survival under aerobic conditions and especially for colonization at the anterior nares, which are the primary ecological niche for *S. aureus* (14). Considering that most of the $PerR_{SA}$ is fully oxidized and no significant further derepression of PerR regulon is triggered by H_2O_2 treatment under aerobic conditions, it is likely that *S. aureus*, as a facultative anaerobic bacterium, has evolved $PerR_{SA}$ to sense low levels of endogenous H_2O_2 normally encountered under aerobic environment, rather than to sense higher levels of external H_2O_2 produced by microbial competitor or by host immune system.

Author Contributions—C. J., J. K., J. H., and J. L. conceived and designed the experiments. C. J., J. K., Y. W., Y. L., T. C., and S. J. performed the experiments. C. J., J. K., H. Y., J. H., and J. L. analyzed the data and wrote the paper.

Acknowledgments—We thank Dr. Joohong Ahnn for help with the C. elegans killing assay and Dr. Cheolju Lee for help with mass spectrometry.

References

1. Imlay, J. A. (2013) The molecular mechanisms and physiological consequences of oxidative stress: lessons from a model bacterium. *Nat. Rev. Microbiol.* **11,** 443–454
2. Imlay, J. A. (2008) Cellular defenses against superoxide and hydrogen peroxide. *Annu. Rev. Biochem.* **77,** 755–776
3. Toledano, M. B., Delaunay, A., Monceau, L., and Tacnet, F. (2004) Microbial H_2O_2 sensors as archetypical redox signaling modules. *Trends Biochem. Sci.* **29,** 351–357
4. Dubbs, J. M., and Mongkolsuk, S. (2012) Peroxide-sensing transcriptional regulators in bacteria. *J. Bacteriol.* **194,** 5495–5503
5. Lee, J. W., and Helmann, J. D. (2007) Functional specialization within the Fur family of metalloregulators. *Biometals* **20,** 485–499
6. Zuber, P. (2009) Management of oxidative stress in *Bacillus*. *Annu. Rev. Microbiol.* **63,** 575–597
7. Lee, J. W., and Helmann, J. D. (2006) The PerR transcription factor senses H_2O_2 by metal-catalysed histidine oxidation. *Nature* **440,** 363–367
8. Traoré, D. A., El Ghazouani, A., Jacquamet, L., Borel, F., Ferrer, J. L., Lascoux, D., Ravanat, J. L., Jaquinod, M., Blondin, G., Caux-Thang, C., Duarte, V., and Latour, J. M. (2009) Structural and functional characterization of 2-oxo-histidine in oxidized PerR protein. *Nat. Chem. Biol.* **5,** 53–59
9. Lowy, F. D. (1998) *Staphylococcus aureus* infections. *N. Engl. J. Med.* **339,** 520–532
10. Horsburgh, M. J., Ingham, E., and Foster, S. J. (2001) In *Staphylococcus aureus*, fur is an interactive regulator with PerR, contributes to virulence, and Is necessary for oxidative stress resistance through positive regulation of catalase and iron homeostasis. *J. Bacteriol.* **183,** 468–475
11. Horsburgh, M. J., Clements, M. O., Crossley, H., Ingham, E., and Foster, S. J. (2001) PerR controls oxidative stress resistance and iron storage proteins and is required for virulence in *Staphylococcus aureus*. *Infect. Immun.* **69,** 3744–3754
12. Morrissey, J. A., Cockayne, A., Brummell, K., and Williams, P. (2004) The staphylococcal ferritins are differentially regulated in response to iron and manganese and via PerR and Fur. *Infect. Immun.* **72,** 972–979
13. Horsburgh, M. J., Wharton, S. J., Cox, A. G., Ingham, E., Peacock, S., and Foster, S. J. (2002) MntR modulates expression of the PerR regulon and superoxide resistance in *Staphylococcus aureus* through control of manganese uptake. *Mol. Microbiol.* **44,** 1269–1286
14. Cosgrove, K., Coutts, G., Jonsson, I. M., Tarkowski, A., Kokai-Kun, J. F., Mond, J. J., and Foster, S. J. (2007) Catalase (KatA) and alkyl hydroperoxide reductase (AhpC) have compensatory roles in peroxide stress resistance and are required for survival, persistence, and nasal colonization in *Staphylococcus aureus*. *J. Bacteriol.* **189,** 1025–1035
15. Lee, J. W., and Helmann, J. D. (2006) Biochemical characterization of the structural Zn^{2+} site in the *Bacillus subtilis* peroxide sensor PerR. *J. Biol. Chem.* **281,** 23567–23578
16. Arnaud, M., Chastanet, A., and Débarbouillé, M. (2004) New vector for efficient allelic replacement in naturally nontransformable, low-GC-content, Gram-positive bacteria. *Appl. Environ. Microbiol.* **70,** 6887–6891
17. Chen, L., Keramati, L., and Helmann, J. D. (1995) Coordinate regulation of *Bacillus subtilis* peroxide stress genes by hydrogen peroxide and metal ions. *Proc. Natl. Acad. Sci. U.S.A.* **92,** 8190–8194
18. Luong, T. T., and Lee, C. Y. (2007) Improved single-copy integration vectors for *Staphylococcus aureus*. *J. Microbiol. Methods* **70,** 186–190
19. Novick, R. P. (1991) Genetic systems in staphylococci. *Methods Enzymol.* **204,** 587–636
20. Charpentier, E., Anton, A. I., Barry, P., Alfonso, B., Fang, Y., and Novick, R. P. (2004) Novel cassette-based shuttle vector system for Gram-positive bacteria. *Appl. Environ. Microbiol.* **70,** 6076–6085
21. Ma, Z., Lee, J. W., and Helmann, J. D. (2011) Identification of altered function alleles that affect *Bacillus subtilis* PerR metal ion selectivity. *Nucleic Acids Res.* **39,** 5036–5044
22. Won, Y. B., Ji, C. J., Cho, J. H., and Lee, J. W. (2010) Mutational analysis of the metal-binding sites of peroxide sensor PerR. *B Korean Chem. Soc.* **31,** 1573–1576
23. Sifri, C. D., Begun, J., Ausubel, F. M., and Calderwood, S. B. (2003) *Caenorhabditis elegans* as a model host for *Staphylococcus aureus* pathogenesis. *Infect. Immun.* **71,** 2208–2217
24. Yang, J. S., Nam, H. J., Seo, M., Han, S. K., Choi, Y., Nam, H. G., Lee, S. J., and Kim, S. (2011) OASIS: online application for the survival analysis of lifespan assays performed in aging research. *PloS One* **6,** e23525
25. Jacquamet, L., Traoré, D. A., Ferrer, J. L., Proux, O., Testemale, D., Hazemann, J. L., Nazarenko, E., El Ghazouani, A., Caux-Thang, C., Duarte, V., and Latour, J. M. (2009) Structural characterization of the active form of PerR: insights into the metal-induced activation of PerR and Fur proteins for DNA binding. *Mol. Microbiol.* **73,** 20–31
26. Traoré, D. A., El Ghazouani, A., Ilango, S., Dupuy, J., Jacquamet, L., Ferrer, J. L., Caux-Thang, C., Duarte, V., and Latour, J. M. (2006) Crystal structure of the apo-PerR-Zn protein from *Bacillus subtilis*. *Mol. Microbiol.* **61,** 1211–1219
27. Needham, A. J., Kibart, M., Crossley, H., Ingham, P. W., and Foster, S. J. (2004) *Drosophila melanogaster* as a model host for *Staphylococcus aureus* infection. *Microbiology* **150,** 2347–2355
28. Prajsnar, T. K., Cunliffe, V. T., Foster, S. J., and Renshaw, S. A. (2008) A novel vertebrate model of *Staphylococcus aureus* infection reveals phagocyte-dependent resistance of zebrafish to non-host specialized pathogens. *Cell. Microbiol.* **10,** 2312–2325
29. Fillat, M. F. (2014) The FUR (ferric uptake regulator) superfamily: diversity and versatility of key transcriptional regulators. *Arch. Biochem. Biophys.* **546,** 41–52
30. Bsat, N., Herbig, A., Casillas-Martinez, L., Setlow, P., and Helmann, J. D. (1998) *Bacillus subtilis* contains multiple Fur homologues: identification of the iron uptake (Fur) and peroxide regulon (PerR) repressors. *Mol. Microbiol.* **29,** 189–198
31. Seaver, L. C., and Imlay, J. A. (2004) Are respiratory enzymes the primary sources of intracellular hydrogen peroxide? *J. Biol. Chem.* **279,** 48742–48750
32. Stone, J. R. (2004) An assessment of proposed mechanisms for sensing hydrogen peroxide in mammalian systems. *Arch. Biochem. Biophys.* **422,** 119–124
33. Aslund, F., Zheng, M., Beckwith, J., and Storz, G. (1999) Regulation of the OxyR transcription factor by hydrogen peroxide and the cellular thiol-disulfide status. *Proc. Natl. Acad. Sci. U.S.A.* **96,** 6161–6165
34. Kim, S., Bang, Y. J., Kim, D., Lim, J. G., Oh, M. H., and Choi, S. H. (2014) Distinct characteristics of OxyR2, a new OxyR-type regulator, ensuring expression of Peroxiredoxin 2 detoxifying low levels of hydrogen peroxide in *Vibrio vulnificus*. *Mol. Microbiol.* **93,** 992–1009
35. Spaan, A. N., Surewaard, B. G., Nijland, R., and van Strijp, J. A. (2013)

Neutrophils *versus Staphylococcus aureus*: a biological tug of war. *Annu. Rev. Microbiol.* **67,** 629–650
36. van Kessel, K. P., Bestebroer, J., and van Strijp, J. A. (2014) Neutrophil-mediated phagocytosis of *Staphylococcus aureus*. *Front. Immunol.* **5,** 467
37. Faulkner, M. J., Ma, Z., Fuangthong, M., and Helmann, J. D. (2012) Derepression of the *Bacillus subtilis* PerR peroxide stress response leads to iron deficiency. *J. Bacteriol.* **194,** 1226–1235
38. Wen, Y. T., Tsou, C. C., Kuo, H. T., Wang, J. S., Wu, J. J., and Liao, P. C. (2011) Differential secretomics of *Streptococcus pyogenes* reveals a novel peroxide regulator (PerR)-regulated extracellular virulence factor mitogen factor 3 (MF3). *Mol. Cell. Proteomics* **10,** M110.007013
39. Duarte, V., and Latour, J. M. (2013) PerR: a bacterial resistance regulator and can we target it? *Future Med. Chem.* **5,** 1177–1179
40. Biasini, M., Bienert, S., Waterhouse, A., Arnold, K., Studer, G., Schmidt, T., Kiefer, F., Cassarino, T. G., Bertoni, M., Bordoli, L., and Schwede, T. (2014) SWISS-MODEL: modelling protein tertiary and quaternary structure using evolutionary information. *Nucleic Acids Res.* **42,** W252–258
41. Varghese, S., Wu, A., Park, S., Imlay, K. R., and Imlay, J. A. (2007) Submicromolar hydrogen peroxide disrupts the ability of Fur protein to control free-iron levels in *Escherichia coli*. *Mol. Microbiol.* **64,** 822–830